

Velocity-independent layer stripping of PP and PS reflection traveltimes

Pawan Dewangan¹ and Ilya Tsvankin²

ABSTRACT

Building accurate interval velocity models is critically important for seismic imaging and AVO (amplitude variation with offset) analysis. Here, we adapt the PP + PS = SS method to develop an exact technique for constructing the interval traveltime-offset function in a target zone beneath a horizontally layered overburden. All layers in the model can be anisotropic, with an essential assumption that the overburden has a horizontal symmetry plane (i.e., up-down symmetry).

Our layer-stripping algorithm is entirely data-driven and, in contrast to the generalized Dix equations, does not require knowledge of the velocity field anywhere in the medium. Important advantages of our approach compared to the Dix-style formalism also include the ability to handle mode-converted waves, long-offset data, and laterally heterogeneous target layers with multiple, curved reflectors. Numerical tests confirm the high accuracy of the algorithm in computing the interval traveltimes of both PP- and PS-waves in a dipping, transversely isotropic layer with a tilted symmetry axis (TTI medium) beneath an anisotropic overburden.

In combination with the inversion techniques developed for homogeneous TTI models, the proposed layer stripping of PP and PS data can be used to estimate the interval parameters of TTI formations in such important exploration areas as the Canadian Foothills. Potential applications of this methodology also include the dip-moveout inversion for the P-wave time-processing parameter η and stable computation of the interval long-spread (nonhyperbolic) moveout for purposes of anisotropic velocity analysis.

INTRODUCTION

Reflection traveltimes are routinely used for reconstructing subsurface velocity fields and imaging target reflectors. However, reflection moveout in general and normal-moveout (NMO) velocity in

particular represent effective quantities that are influenced by the medium properties along the entire raypath of the reflected wave. Therefore, interval parameter estimation for purposes of prestack and poststack migration requires application of layer-stripping (e.g., Dix, 1955; Liu, 1997; Grechka and Tsvankin, 2000; Sarkar and Tsvankin, 2004) or tomographic (e.g., Stork, 1991; Grechka et al., 2002a,b) methods. Layer parameters are also needed, for example, in AVO analysis, seismic-fracture characterization, and lithology discrimination.

In horizontally layered, isotropic media, the NMO velocity of reflected waves is equal to the root-mean-square (RMS) of the interval velocities (Dix, 1955). This simple relationship helps to obtain the interval velocity using the NMO velocities for the reflections from the top and bottom of the layer. A more general version of the Dix equation for isotropic models with dipping interfaces was presented by Shah (1973).

If the medium is transversely isotropic with a vertical-symmetry axis (VTI) and laterally homogeneous, NMO velocity is still equal to the RMS of the interval NMO velocities (Hake et al., 1984). However, since the interval NMO velocity is distorted by anisotropy parameters, application of the Dix equation does not yield the true interval vertical velocities, which causes mis-ties in time-to-depth conversion (e.g., Tsvankin, 2005). For wide-azimuth, pure-mode (nonconverted) data acquired above a stack of horizontal, arbitrarily anisotropic layers, the exact NMO velocity can be obtained by Dix-type averaging of the interval NMO ellipses (Grechka et al., 1999). On the whole, as long as the model is laterally homogeneous, the interval NMO velocity or interval NMO ellipse can still be computed using just the conventional-spread moveout of reflection events from the top and bottom of the layer of interest.

Dix-type averaging of the interval NMO velocities remains valid even for reflections from dipping interfaces in anisotropic media, if the CMP (common-midpoint) line is confined to a vertical symmetry plane and the overburden is laterally homogeneous (Alkhalifah and Tsvankin, 1995; Tsvankin, 2005; see Figure 1). A 3D extension of this result to the NMO ellipses of dipping events is given by Grechka et al. (1999) and Grechka and Tsvankin (2002a). The main difference between these generalized Dix equations and the conventional

Manuscript received by the Editor August 2, 2005; revised manuscript received November 22, 2005; published online July 28, 2006.

¹Formerly Center for Wave Phenomena, Department of Geophysics, Colorado School of Mines, Golden, Colorado 80401-1887; presently Geological Oceanography Division, National Institute of Oceanography, Dona Paula, Goa-403004, India. E-mail: pdewangan@darya.nio.org.

²Center for Wave Phenomena, Department of Geophysics, Colorado School of Mines, Golden, Colorado 80401-1887. E-mail: ilya@dix.mines.edu.

© 2006 Society of Exploration Geophysicists. All rights reserved.

Dix formula is in the nature of the interval NMO velocity or the interval NMO ellipse. If the reflector is dipping, the NMO velocity in each layer no longer corresponds to any physical interface and must be computed for a nonhorizontal (imaginary) reflector orthogonal to the slowness vector of the zero-offset ray in this layer (Figure 1).

Although this requirement does not pose problems in forward modeling, it causes serious difficulties in interval parameter estimation, because recorded reflections from the overburden yield only the NMO velocities for horizontal interfaces. Therefore, velocity-analysis algorithms based on the generalized Dix equations involve interval parameter estimation for the whole overburden. When the medium is anisotropic, the Dix-type layer stripping of NMO velocities or ellipses usually requires reflections from both horizontal and dipping events for each depth interval (Alkhalifah and Tsvankin, 1995; Grechka and Tsvankin, 2000).

The more general tomographic algorithms for anisotropic media (Le Stunff and Jeannot, 1998; Williamson et al., 1999) do not employ layer stripping explicitly, but they also rely on the velocity model of the overburden in reconstructing the deeper part of the section. Therefore, tomographic velocity estimates are sensitive to errors in the overburden parameters, and tomographic models suffer from error accumulation with depth. Redataming techniques based on the common-focus-point technology do not require accurate velocities in the overburden, but they use complicated updating procedures in the migrated domain and are implemented only for P-waves in isotropic media (Kelamis et al., 2002).

Another principal limitation of the generalized Dix equations and other algorithms operating with NMO velocity is the assumption of symmetric reflection moveout (i.e., the traveltimes stay the same when the source and receiver are interchanged). While this assumption is always satisfied for pure (nonconverted) modes, the moveout of PS- or SP-waves is symmetric only in laterally homogeneous media with a horizontal plane of symmetry. Dewangan and Tsvankin (2006a, b) showed that the asymmetric moveout of PS waves in TI media with a tilted symmetry axis (TTI) provides critically important information for anisotropic parameter estimation. Their inversion algorithm, however, is developed for a single horizontal or dip-

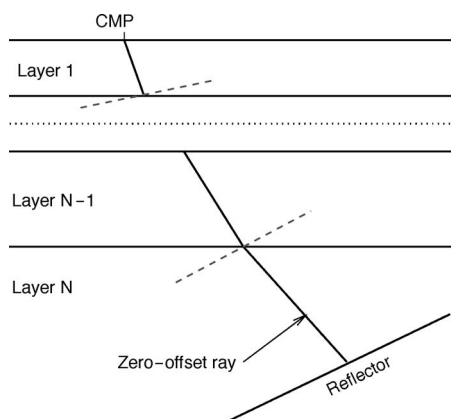


Figure 1. 2D anisotropic model used by Alkhalifah and Tsvankin (1995) in the derivation of their generalized Dix equation. The dipping reflector is overlaid by a laterally homogeneous medium, and the acquisition line is confined to the reflector dip plane that coincides with a symmetry plane in all layers. The NMO velocity at the surface is equal to the RMS of the interval NMO velocities computed for imaginary interfaces (dashed lines) orthogonal to the slowness vector of the zero-offset ray (equation 1).

ping TTI layer and cannot be applied to layered media using existing Dix-type formalism.

Finally, the generalized Dix equations for NMO velocities describe only conventional-spread moveout for the maximum offset-to-depth ratio not much larger than unity. Similar averaging expressions for long-offset data involve the quartic moveout coefficient and are limited to horizontally layered models (e.g., Tsvankin and Thomsen, 1994; Alkhalifah, 1997; Al-Dajani and Tsvankin, 1998).

Here, we present a technique for computing the exact interval traveltimes and the corresponding offsets of pure-mode and converted waves in a heterogeneous target zone overlaid by a laterally homogeneous overburden. Our approach is based on the PP + PS = SS method originally designed for generating pure-mode, SS reflection data from PP- and PS-waves (Grechka and Tsvankin, 2002b; Grechka and Dewangan, 2003). Application of the PP + PS = SS method makes it possible to perform layer stripping without knowledge of the medium parameters in the overburden. We begin by introducing the layer-stripping algorithm for pure modes and then generalize it for converted waves. The accuracy of the estimated interval moveouts for both PP- and PS-waves is verified by numerical testing on layered TI models with the depth-varying tilt of the symmetry axis. Although the method is introduced in 2D, it can be extended to 3D, wide-azimuth data.

LAYER STRIPPING FOR PURE REFLECTION MODES

Let us consider pure (nonconverted) reflected waves in a possibly anisotropic medium comprised of a laterally homogeneous overburden above a heterogeneous target zone (Figure 2). To make the problem 2D, the acquisition line is assumed to coincide with a vertical symmetry plane in all layers. Therefore, the incidence plane represents a symmetry plane for the model as a whole.

The target zone (i.e., the layer between the reflector and the bottom of the overburden) can be arbitrarily heterogeneous in the incidence plane. In particular, the target zone can include multiple, curved interfaces above the reflector. The only restriction on the type of anisotropy in the target zone is that the incidence plane must be a plane of symmetry. Note that this restriction, which is needed to

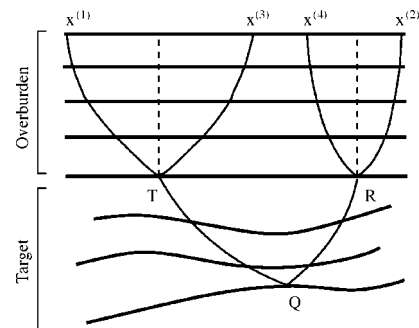


Figure 2. 2D ray diagram of the layer-stripping algorithm for pure-wave reflection modes. Points T and R are located at the bottom of the laterally homogeneous overburden; each layer in the overburden is also assumed to have a horizontal symmetry plane. The target reflection ($x^{(1)}$ TQR $x^{(2)}$) and the reflection from the bottom of the overburden ($x^{(1)}$ T $x^{(3)}$) share the same downgoing leg ($x^{(1)}$ T). The upgoing leg of the target event (R $x^{(2)}$) coincides with a leg of another overburden reflection, $x^{(2)}$ R $x^{(4)}$. The layer-stripping algorithm can be applied in the same way to any other reflector in the target zone.

make wave propagation 2D, can be lifted in the 3D version of our method operating with wide-azimuth data. Although such an extension is not discussed here, it can be based on the 3D implementation of the PP + PS = SS method (Grechka and Tsvankin, 2002b).

Each layer in the overburden, however, is assumed to be laterally homogeneous with a horizontal symmetry plane. Under these assumptions, any reflection point at the bottom of the overburden (e.g., points T and R in Figure 2) coincides with the CMP for the corresponding source-receiver pair, and the traveltimes along the upgoing and downgoing segments of the reflected ray are equal to each other.

For the special case of a laterally homogeneous target zone, the NMO velocity in our model can be found from the following 2D, Dix-type equation (Alkhalifah and Tsvankin, 1995; Tsvankin, 2005):

$$V_{\text{nmo}}^2(N) = \frac{1}{t_0} \sum_{i=1}^N [V_{\text{nmo}}^{(i)}(p)]^2 t_0^{(i)}(p), \quad (1)$$

where N is the number of layers above the reflector, t_0 is the zero-offset traveltime, $t_0^{(i)}$ is the interval traveltime along the zero-offset ray in layer i , $V_{\text{nmo}}^{(i)}$ is the interval NMO velocity, and p is the ray parameter (horizontal slowness) of the zero-offset ray. Note that the reflector curvature has no influence on $V_{\text{nmo}}(N)$, because NMO velocity is independent of reflection-point dispersal (Hubral and Krey, 1980).

As discussed above, the interval NMO velocity in equation 1 must be computed for an imaginary reflector orthogonal to the slowness vector of the zero-offset ray in each layer (Figure 1). Therefore, estimation of the NMO velocity in layer N from equation 1 generally involves inversion for the relevant medium parameters in the whole overburden (Alkhalifah and Tsvankin, 1995). The layer-stripping methodology described below makes this requirement unnecessary.

Layer-stripping algorithm

Here, we demonstrate that a variation of the PP + PS = SS method (Grechka and Tsvankin, 2002b; Grechka and Dewangan, 2003) can be used to obtain the exact interval traveltime-offset function in the target layer. This can be accomplished by combining the target reflection with the ones from the bottom of the overburden in such a way that they share the same ray segments in the whole overburden (Figure 2).

Suppose the event of interest was excited at location $x^{(1)}$ and recorded at location $x^{(2)}$ (or vice versa), and the reflection from the bottom of the overburden was acquired for a sufficiently wide range of source-receiver offsets. Following the methodology of Grechka and Tsvankin (2002b), we can form a common-receiver gather of the target event $x^{(1)}\text{TQR } x^{(2)}$ at point $x^{(2)}$ and determine the time slope on this gather at point $x^{(1)}$. Since the slowness vector is equal to the gradient of the traveltime surface, the estimated time slope coincides with the ray parameter (horizontal slowness) of the reflection $x^{(1)}\text{TQR } x^{(2)}$ at the source location $x^{(1)}$. We then use the same algorithm to evaluate the time slopes of the overburden reflections excited at $x^{(1)}$ and recorded at different locations along the line. For a certain receiver location $x^{(3)}$, the time slope (ray parameter) of the overburden reflection from $x^{(1)}$ to $x^{(3)}$ coincides with that of the target event,

$$\frac{\partial t^{\text{eff}}(x^{(1)}, x^{(2)})}{\partial x^{(1)}} = \frac{\partial t^{\text{ovr}}(x^{(1)}, x^{(3)})}{\partial x^{(1)}}, \quad (2)$$

where the superscripts *eff* and *ovr* refer, respectively, to the reflection traveltimes from the target (i.e., the effective traveltime) and

from the bottom of the overburden. The identical ray parameters mean that the reflections $x^{(1)}\text{TQR } x^{(2)}$ and $x^{(1)}\text{T}x^{(3)}$ share the same downgoing leg $x^{(1)}\text{T}$ in the overburden (Figure 2).

Repeating this procedure at point $x^{(2)}$ and matching the time slopes,

$$\frac{\partial t^{\text{eff}}(x^{(2)}, x^{(1)})}{\partial x^{(2)}} = \frac{\partial t^{\text{ovr}}(x^{(2)}, x^{(4)})}{\partial x^{(2)}}, \quad (3)$$

we find the overburden reflection $x^{(2)}\text{R}x^{(4)}$ that has the same upgoing leg $\text{R}x^{(2)}$ as the target event $x^{(1)}\text{TQR } x^{(2)}$.

Since the overburden is laterally homogeneous and has a horizontal symmetry plane, the raypath of any pure mode reflected from the bottom of the overburden is symmetric with respect to the reflection point. Therefore, the interval traveltime in the target layer can be expressed as

$$t^{\text{int}}(T, R) = t^{\text{eff}}(x^{(1)}, x^{(2)}) - \frac{1}{2} [t^{\text{ovr}}(x^{(1)}, x^{(3)}) + t^{\text{ovr}}(x^{(2)}, x^{(4)})]. \quad (4)$$

The symmetry of the reflection raypath in the overburden also implies that the interval traveltime is obtained for the source-receiver pair (T, R) with the horizontal coordinates

$$x_T = \frac{x^{(1)} + x^{(3)}}{2}, \quad x_R = \frac{x^{(2)} + x^{(4)}}{2}. \quad (5)$$

The depth of the bottom of the overburden (i.e., of points T and R) cannot be found prior to parameter estimation. Velocity analysis in the target layer, however, does not require the actual depth positioning of the sources and receivers after the layer stripping.

Note that the algorithm outlined above can be applied independently to any reflector in the target zone, essentially performing kinematic downward continuation of the wavefield through a laterally homogeneous overburden. As in the PP + PS = SS method, this continuation procedure does not require knowledge of the velocity model and is not restricted to isotropic media. In contrast to the Dix-type equation 1, our method can be applied to long-offset data and can handle a laterally heterogeneous target layer.

Numerical example

The layer-stripping algorithm was tested on PP reflection data generated for the layered TI model in Figure 3, where the target zone is represented by the dipping TTI layer. The traveltimes from the plane dipping reflector and the bottom of the overburden (i.e., the bottom of the second VTI layer) were computed by anisotropic ray tracing with a shot spacing of 25 m and a receiver spacing of 50 m (Figure 4). To satisfy the 2D assumption of the algorithm, the incidence plane coincides with the dip plane of the reflector and contains the symmetry axis of the TTI layer.

In our implementation of the layer stripping, we follow the original version of the PP + PS = SS method by Grechka and Tsvankin (2002b) based on equalizing reflection slopes (see above). For given source and receiver locations $x^{(1)}$ and $x^{(2)}$, substitution of the estimated coordinates $x^{(3)}$ and $x^{(4)}$ into equation 4 yields the interval traveltime in the target layer for the source and receiver located at points T and R (Figure 2). Although the depth of the top of the target layer remains unknown, the goal of the layer stripping is achieved by obtain-

ing the horizontal source/receiver coordinates (equation 5) needed to construct the interval traveltime function.

By repeating the above procedure to cover the whole recorded range of the source-receiver offsets for the dipping event, we compute the interval PP-wave traveltime for a number of the corresponding source/receiver pairs. These pairs do not necessarily form a CMP, common-shot, or common-receiver gather, and need to be sorted to analyze the interval traveltime in any desired configuration. This represents a minor complication compared with the original PP + PS = SS method, in which the type of the output gather can be specified in advance.

To verify the accuracy of the layer stripping, we computed the interval PP-wave traveltime in the dipping layer and the corresponding source/receiver coordinates directly, using ray tracing. The agreement between our method and the ray-tracing results is excellent (Figures 5 and 6). This and other synthetic tests we performed for a representative set of layered TI models confirm that the layer-stripping algorithm is exact and can be applied for large source-receiver offsets.

LAYER STRIPPING FOR MODE-CONVERTED WAVES

In contrast to the generalized Dix equations, our layer-stripping algorithm can be easily adapted for mode-converted (PS or SP)

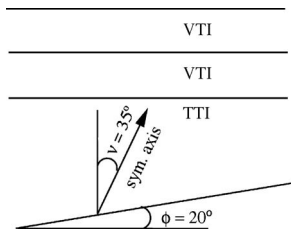


Figure 3. Transversely isotropic model used to test the layer-stripping algorithm. The first layer has a vertical symmetry axis (VTI medium) and the following parameters: the symmetry-direction P-wave velocity $V_{p0} = 2$ km/s; the symmetry-direction S-wave velocity $V_{s0} = 1$ km/s; the thickness $h = 0.25$ km; and Thomsen's anisotropy parameters $\epsilon = 0.2$ and $\delta = 0.1$. The second layer is also VTI with $V_{p0} = 4$ km/s, $V_{s0} = 2$ km/s, $h = 0.25$ km, $\epsilon = 0.15$, and $\delta = 0.05$. The third (target) layer is dipping TTI with the symmetry axis tilted at $\nu = 35^\circ$, the dip of the bottom $\phi = 20^\circ$, $V_{p0} = 4$ km/s, $V_{s0} = 2$ km/s, $h = 0.5$ km, $\epsilon = 0.25$, and $\delta = -0.05$. Thomsen's parameters in the TTI layer are defined with respect to the symmetry axis (Dewangan and Tsvankin, 2006a,b).

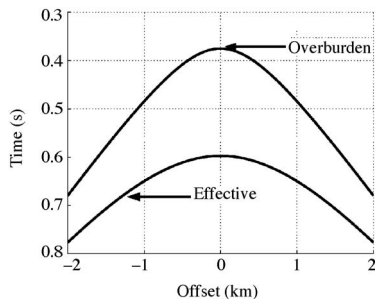


Figure 4. CMP gathers of the PP-wave reflections from the bottom of the second layer (marked as *overburden*) and from the dipping reflector (marked as *effective*) for the model in Figure 3. The traveltimes were generated by an anisotropic ray-tracing code.

waves. With the same model assumptions as those used above for pure modes, we consider a PS-wave converted at the target reflector (Figure 7). Since the upgoing leg of the PS mode represents a shear wave, the algorithm must operate with both PP- and SS-waves reflected from the bottom of the overburden. In the absence of shear-wave excitation, the needed reflection moveout of SS-waves can be obtained by applying the PP + PS = SS method to the PP and PS reflections from the bottom of the overburden.

Layer-stripping algorithm

As in the previous section, the target reflection event has the ray-path $x^{(1)}TQRx^{(2)}$, but now the downgoing leg represents a P-wave, while the upgoing leg is an S-wave (Figure 7). By matching the time slopes at point $x^{(1)}$, we identify the overburden PP-wave reflection $x^{(1)}Tx^{(3)}$ that shares the segment $x^{(1)}T$ with the target PS event. The same procedure at point $x^{(2)}$ yields the reflected SS-wave $x^{(4)}Rx^{(2)}$ that has the same shear-wave segment $Rx^{(2)}$ as the PS wave. Both events (PP and SS) from the bottom of the overburden have symmetric raypaths with respect to their reflection points. Thus, the source/receiver coordinates (i.e., the horizontal coordinates of points T and R) for the PS wave propagating in the target layer can be found from equation 5, while the interval PS-wave traveltime is expressed as

$$t_{PS}^{int}(T,R) = t_{PS}^{eff}(x^{(1)},x^{(2)}) - \frac{1}{2} [t_{PP}^{ovr}(x^{(1)},x^{(3)}) + t_{SS}^{ovr}(x^{(2)},x^{(4)})]. \tag{6}$$

Our implementation of this layer-stripping algorithm for PS-waves is similar to that described above for PP-waves.

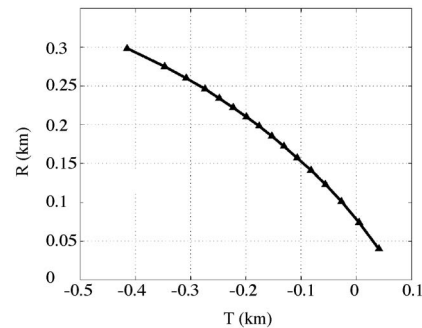


Figure 5. Source and receiver coordinates at the top of the target TTI layer obtained from the ray-traced data for the model in Figure 3. Here and in Figure 6, the triangles mark the output of the layer-stripping algorithm; the solid line is the result of ray tracing.

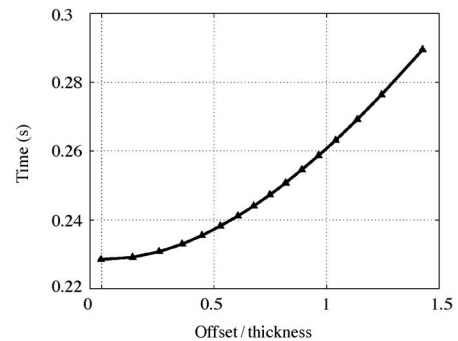


Figure 6. Interval PP-wave traveltime in the target layer as a function of offset for the source/receiver pairs from Figure 5.

Numerical examples

Noise-free test

Figure 8 shows ray-traced CMP gathers of the target PS event and the pure-mode reflections from the bottom of the overburden for the model in Figure 3. Note that the PS-wave moveout is asymmetric (i.e., the traveltime is different for positive and negative offsets), because of the combined influence of reflector dip ($\phi = 20^\circ$) and the tilt of the symmetry axis ($\nu = 35^\circ$) in the target TTI layer. This moveout asymmetry, however, does not pose a problem for our layer-stripping method, which relies only on the symmetry of reflection raypaths in the overburden.

The layer-stripped, interval PS-wave traveltimes and the corresponding source/receiver coordinates are close to the exact values computed by ray tracing (Figures 9 and 10). The minor deviations from the ray-tracing results are caused by interpolation errors related to the finite source and receiver sampling. Since the TTI layer is the only source of moveout asymmetry in the model, the interval traveltimes in Figure 10 exhibit a more significant asymmetry than do the effective traveltimes in Figure 8. The PS-wave moveout function for the target layer, supplemented by the interval PP-wave moveout, can serve as the input to the inversion algorithm of Dewangan and Tsvankin (2006b), which is designed to estimate the parameters of dipping TTI layers.

Test on noise-contaminated data

The PP + PS = SS method has been successfully applied to synthetic data contaminated by noise (Grechka and Tsvankin, 2002b), as well as to field data (e.g., Grechka and Dewangan, 2003). Still, it is essential to verify the stability of the proposed layer-stripping algorithm in the presence of noise.

To simulate time-picking errors, we added Gaussian noise with a standard deviation of 10 ms to the input traveltimes used in the above test for PS-waves (Figures 8–10). As discussed by Grechka and Tsvankin (2002b), random picking errors may cause substantial distortions in the estimated time slopes. To reduce this instability, we fitted a polynomial function to the noise-contaminated traveltimes. The layer-stripping algorithm was applied for multiple realizations of the noise to calculate the mean values and standard deviations of

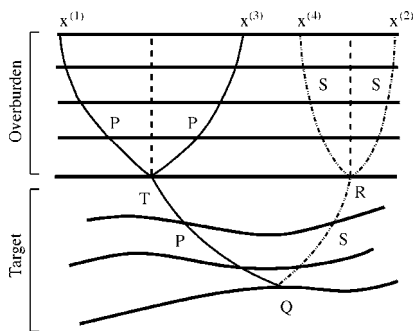


Figure 7. 2D ray diagram of the layer-stripping algorithm for PS-waves. The model is the same as that in Figure 2, with the overburden composed of laterally homogeneous layers with a horizontal symmetry plane. The target PS reflection ($x^{(1)}TQRx^{(2)}$) and the PP reflection from the bottom of the overburden ($x^{(1)}Tx^{(3)}$) share the same downgoing leg ($x^{(1)}T$). The upgoing leg of the target PS event ($Rx^{(2)}$) coincides with a leg of the overburden SS reflection $x^{(2)}Rx^{(4)}$.

the output parameters (Figures 11 and 12). Evidently, despite the relatively high level of noise, our algorithm produces unbiased results, and time errors are not amplified by the layer-stripping procedure. Such error amplification, however, cannot be avoided if the target horizon has a much smaller thickness than the overburden.

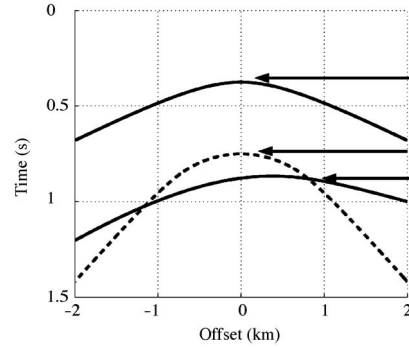


Figure 8. CMP gathers of reflected waves for the model in Figure 3 computed by anisotropic ray tracing. The PS-wave is converted at the dipping interface, while the PP- and SS-waves are reflected from the bottom of the overburden. The offset is positive when the source-to-receiver vector points downdip.

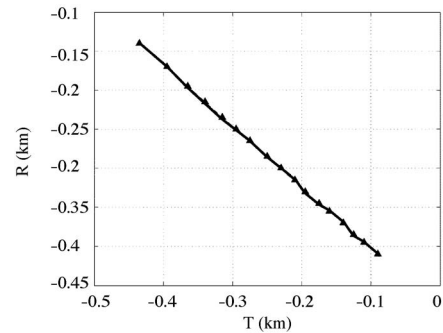


Figure 9. Source and receiver coordinates of the PS-wave at the top of the target TTI layer obtained from ray-traced data (PP-, PS-, and SS-waves) for the model in Figure 3. Here and in Figure 10, the triangles mark the output of the layer-stripping algorithm; the solid line is the result of ray tracing.

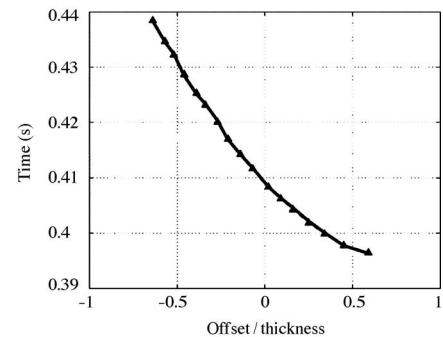


Figure 10. Interval PS-wave traveltime in the target layer as a function of offset for the source/receiver pairs from Figure 9.

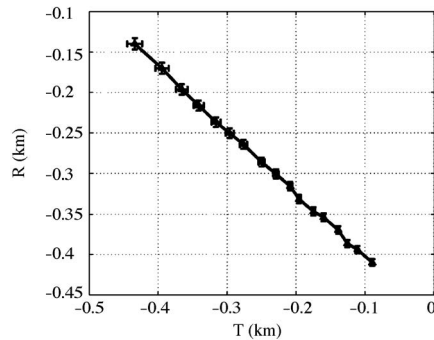


Figure 11. Source and receiver coordinates of the PS-wave at the top of the target TTI layer (see Figure 9) for noise-contaminated input data. Here and in Figure 12, the triangles mark the mean values of the quantities computed by the layer-stripping algorithm; the solid line is the result of ray tracing. The error bars correspond to the standard deviation in each quantity; the standard deviation of the Gaussian noise added to the input traveltimes is 10 ms.

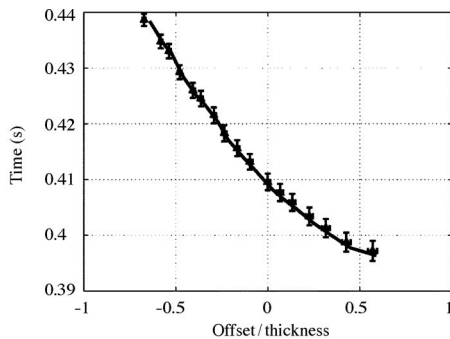


Figure 12. Interval PS-wave traveltime in the target layer as a function of offset for the source/receiver pairs from Figure 11. The input data were contaminated with Gaussian noise; the results of the noise-free test are shown in Figure 10.

CONCLUSIONS

The principle of the PP + PS = SS method can be used to carry out exact layer stripping for both pure and mode-converted waves in anisotropic media. The main assumptions of the algorithm introduced here are that the overburden is laterally homogeneous and has a horizontal symmetry plane (i.e., up-down symmetry) in each layer. The target layer, however, can be laterally heterogeneous without up-down symmetry, although in the 2D version of the method, the incidence plane must coincide with a symmetry plane for the whole model.

Under these assumptions, simple operations with reflection traveltimes originally employed in the PP + PS = SS method help to identify the overburden events that share the downgoing and upgoing legs with the target reflection. This allows us to perform kinematic downward continuation of the wavefield and build the interval traveltime-offset function without knowledge of the medium parameters. Numerical examples for layered TI media above a dipping reflector confirm that the algorithm gives exact results for both pure and converted modes. Although the testing was limited to PP and PS

waves, the methodology can be also applied to SS and SP reflections excited by shear sources.

Allowance for lateral heterogeneity in the target zone, for mode conversions along the raypath, and for nonhyperbolic moveout makes our algorithm much more general than the Dix-type equations for NMO velocity.¹ It should be emphasized that our method can yield exact long-offset interval traveltimes of reflections from dipping and curved interfaces. Note that existing layer-stripping techniques for long-offset data are derived for the quartic moveout coefficient in layer-cake models and cannot account for reflector dip. Although tomographic methods can also handle long-spread data from heterogeneous media, our layer stripping is velocity-independent, and the computed interval moveouts are not influenced by errors in the overburden parameters.

Since our algorithm operates with individual traveltimes, it is more complicated and computer-intensive than layer stripping of NMO velocities. Hence, if the velocity model of the overburden is known and only conventional-spread, P-wave data are available, it is more efficient to apply Dix-type techniques.

EXTENSIONS AND APPLICATIONS

The 2D algorithm discussed here can be extended to wide-azimuth surveys using the 3D version of the PP + PS = SS method described by Grechka and Tsvankin (2002b) and Grechka and Dewangan (2003). For multiazimuth data, identifying the target and overburden reflections with the same ray segments requires estimating the two horizontal slowness components (time slopes). The 3D version of our method removes all restrictions on the anisotropy and heterogeneity of the target layer, and the overburden no longer needs to have a vertical symmetry plane.

An important application of our results is in velocity analysis for TTI layers using multicomponent (PP and PS) data. As shown by Dewangan and Tsvankin (2006a, b), the combination of the asymmetry attributes of PS-waves with pure-mode moveout signatures can provide sufficient information for parameter estimation in a homogeneous TTI medium. The layer-stripping algorithm introduced here makes it possible to implement this inversion technique for realistic models with a stratified overburden above the target TTI zone.

Our method also overcomes the limitations of the generalized Dix equations in the dip-moveout inversion for the P-wave time-processing parameter η in VTI media. Because of the need to compute the interval NMO velocities in the overburden for nonexistent reflectors, Dix-type algorithms designed to estimate η using dipping events rely on the presence of both horizontal and dipping interfaces in each layer (Alkhalifah and Tsvankin, 1995; Tsvankin, 2005). This requirement, which is often difficult to satisfy in practice, is no longer needed if the interval moveout is computed by the velocity-independent, layer-stripping technique.

It can also be highly beneficial to apply our algorithm in the inversion of nonhyperbolic moveout for anisotropic media. In principle, the interval quartic-moveout coefficient A_4 (and, for P-waves, the interval parameter η) in layer-cake VTI media can be estimated from the effective values of A_4 for the top and bottom of the layer (Tsvankin and Thomsen, 1994; Alkhalifah, 1997). This operation, however, suffers from instability caused by the tradeoff between the effective A_4 and NMO velocity and by the subsequent error amplification in the computation of the interval η values (Tsvankin, 2005).

¹The Dix equations, however, do not require up-down symmetry in the overburden.

The layer-stripping technique presented here, which is not influenced by errors in the moveout coefficients, can produce accurate interval long-spread traveltimes, which can then be inverted for the parameter η . Moreover, the 3D version of our method can increase the accuracy of interval parameter estimation based on nonhyperbolic moveout for more complicated, azimuthally anisotropic models.

ACKNOWLEDGMENTS

We are grateful to members of the A(nisotropy)-Team of the Center for Wave Phenomena (CWP), Colorado School of Mines, for useful discussions and to the editors and reviewers of *GEOPHYSICS* for constructive comments and suggestions. The support for this work was provided by the Consortium Project on Seismic Inverse Methods for Complex Structures at CWP and by the Chemical Sciences, Geosciences and Biosciences Division, Office of Basic Energy Sciences, Office of Science, U. S. Department of Energy.

REFERENCES

- Al-Dajani, A., and I. Tsvankin, 1998, Nonhyperbolic reflection moveout for horizontal transverse isotropy: *Geophysics*, **63**, 1738–1753.
- Alkhalifah, T., 1997, Velocity analysis using nonhyperbolic moveout in transversely isotropic media: *Geophysics*, **62**, 1839–1854.
- Alkhalifah, T., and I. Tsvankin, 1995, Velocity analysis in transversely isotropic media: *Geophysics*, **60**, 1550–1566.
- Dewangan, P., and I. Tsvankin, 2006a, Modeling and inversion of PS-wave moveout asymmetry for tilted TI media: Part I — Horizontal TTI layer: *Geophysics* (this issue).
- , 2006b, Modeling and inversion of PS-wave moveout asymmetry for tilted TI media: Part II — Dipping TTI layer: *Geophysics* (this issue).
- Dix, C. H., 1955, Seismic velocities from surface measurements: *Geophysics*, **20**, 68–86.
- Grechka, V., and P. Dewangan, 2003, Generation and processing of pseudo shear-wave data: Theory and case study: *Geophysics*, **68**, 1807–1816.
- Grechka, V., A. Pech, and I. Tsvankin, 2002a, P-wave stacking-velocity tomography for VTI media: *Geophysical Prospecting*, **50**, 151–168.
- Grechka, V., and I. Tsvankin, 2000, Inversion of azimuthally dependent NMO velocity in transversely isotropic media with a tilted axis of symmetry: *Geophysics*, **65**, 232–246.
- , 2002a, NMO-velocity surfaces and Dix-type formulas in anisotropic heterogeneous media: *Geophysics*, **67**, 939–951.
- , 2002b, PP + PS = SS: *Geophysics*, **67**, 1961–1971.
- , 2002b, Multicomponent stacking-velocity tomography for transversely isotropic media: *Geophysics*, **67**, 1564–1574.
- Grechka, V., I. Tsvankin, and J. K. Cohen, 1999, Generalized Dix equation and analytic treatment of normal-moveout velocity for anisotropic media: *Geophysical Prospecting*, **47**, 117–148.
- Hake, H., K. Helbig, and C. S. Mesdag, 1984, Three-term Taylor series for $t^2 - x^2$ curves over layered transversely isotropic ground: *Geophysical Prospecting*, **32**, 828–850.
- Hubral, P., and T. Krey, 1980, Interval velocities from seismic reflection time measurements: SEG.
- Kelamis, P. G., K. E. Erickson, D. J. Verschuur, and A. J. Berkhout, 2002, Velocity-independent redatuming: A new approach to the near-surface problem in land seismic data processing: *The Leading Edge*, **21**, 730–735.
- Le Stunff, Y., and J. P. Jeannot, 1998, Pre-stack anisotropic depth imaging: 60th EAGE Conference, Extended Abstracts, Paper No. 5-21.
- Liu, Z., 1997, An analytical approach to migration velocity analysis: *Geophysics*, **62**, 1238–1249.
- Sarkar, D., and I. Tsvankin, 2004, Migration velocity analysis in factorized VTI media: *Geophysics*, **69**, 708–718.
- Shah, P. M., 1973, Use of wavefront curvature to relate seismic data with subsurface parameters: *Geophysics*, **38**, 812–825.
- Stork, C., 1991, Reflection tomography in the post migrated domain: *Geophysics*, **57**, 680–692.
- Tsvankin, I., 2005, *Seismic signatures and analysis of reflection data in anisotropic media*, 2nd ed.: Elsevier Science Publishing Company, Inc.
- Tsvankin, I., and L. Thomsen, 1994, Nonhyperbolic reflection moveout in anisotropic media: *Geophysics*, **59**, 1290–1304.
- Williamson, P., P. Berthet, J. Mispel, and P. Sexton, 1999, Anisotropic velocity model construction and migration: An example from West Africa: 69th Annual International Meeting, SEG, Expanded Abstracts, 1592–1595.